M dwarfs, L dwarfs, T dwarfs and subdwarfs: $\Psi(M)$ at and below the hydrogen-burning limit

Reid, I. Neill(1) ; [1]University of Pennsylvania, Philadelphia, PA 19104
Email (INR): inr@herschel.physics.upenn.edu

Abstract

Eighty percent of the stars within the immediate Solar Neighbourhood are M dwarfs, and low mass stars make a correspondingly large contribution to the stellar mass budget. Until recently, the mass density due to substellar mass brown dwarfs was a matter for speculation, but results from the new generation of near-infrared sky surveys (DENIS and 2MASS), supplemented by deeper optical/far-red surveys (POSS II and, most recently, SDSS) have revolutionised this area of research. I review these new observational discoveries and consider their interpretation in the light of recent theoretical models. I consider the conclusions which can be drawn regarding the likely form of the stellar/sub-stellar mass function for the Galactic disk, and compare those results against recent determinations of the mass function in the Galactic halo.

1 Introduction

Eldredge and Gould's theory of punctuated equilibrium envisages biological evolution as long periods of near stasis interspersed with short bursts of frenzied activity. Whether punc. equ. is the most appropriate evolutionary model is outwith the bounds of this article, but it provides an apt description of scientific progress in some fields. In particular, for those of us working on low mass stars and brown dwarfs, the last few years have seen equilibrium well and truly punctuated. Within a span of five years we have progressed from arguing about whether substellar-mass brown dwarfs actually exist, to devising not just one, but two, new spectral classifications to deal with a plethora of unequivocal examples. This review summarises some of these new developments, concentrating on observational and theoretical studies of the general field population. In particular, I consider the constraints which can be set on the form of the stellar and substellar mass function, $\Psi(M)$, for the Galactic disk, and compare those results with the most recent estimates of $\Psi(M)$ for the (stellar) Galactic halo.

2 Finding brown dwarfs

Surveys for very low-mass (VLM) dwarfs can be grouped under two basic headings: photometric scans for isolated objects with extreme colours in either star clusters or the general field; and searches for faint companions to known nearby stars. prior to the 1990s, the overwhelming majority of those surveys were based on photographic plate material, using either high proper motion or red colours to identify nearby late-type dwarfs. Limited to wavelengths shortward of $1\mu m$ and magnitudes fainter than 20th, those techniques are ill-suited to finding ultracool dwarfs, particularly brown dwarfs, which offer the added complication of short visible lifetimes due to the absence of hydrogen fusion as a central energy source. Higher quantum efficiency, red-sensitive CCDs and near-infrared arrays have proven more effective tools, as discussed further below. Three key early observations should be highlighted as harbingers of the recent dramatic progress.

2.1 Early results

The Pleiades cluster: surveys for brown dwarfs in clusters have the advantage that age is a (relatively) known quantity, and searches can be targeted to the appropriate colour/magnitude régime. The relative youth of the Pleiades, and consequent higher luminosities of brown dwarfs, supply an additional advantage. The first deep CCD-based surveys for VLM Pleiads were undertaken by Stauffer et al (1989, 1994) using the Palomar 200-inch, and resulted in the identification of several candidates lying on the extension of the cluster main-sequence - notably PPl 15. Similar surveys covering a larger fraction of the cluster have since been undertaken by the Tenerife group (Rebolo, Martín, Magazzu, Zapatero Osorio and collaborators) and many fainter brown dwarf candidates have been identified (see Zapatero Osorio et al, 1996).

The Tenerife group is also responsible for identifying one of the few available methods of discriminating (some) brown dwarfs from VLM stars: detection of Li 6708Å absorption, the lithium test (Rebolo et al, 1992). Degeneracy dictates that VLM dwarfs and brown dwarfs have nearly identical radii, and therefore nearly identical luminosities at the same effective temperature. Brown dwarfs with masses below $0.06M_\odot$ never achieve central temperatures exceeding $\sim 2.5 \times 10^6$K, the critical temperature for lithium burning. Thus, even though those objects are fully convective during their evolution through spectral type M, the reservoir of primordial lithium remains intact, while higher-mass brown dwarfs and stars deplete lithium.

High resolution spectroscopy of PPl 15 by Basri & Marcy (1994) detected lithium, identifying the object as a brown dwarf, but with surprisingly high luminosity. Subsequent observations (Basri & Martín, 1997) revealed PPl 15 to be a double-lined spectroscopic binary, with near equal-mass $\sim 0.06M_\odot$ components. recently, Stauffer et al (1998) have demonstrated that low-mass Pleiads confirm the lithium-depletion theory, with all dwarfs of spectral type later than M6 having detectable lithium, In the field, any dwarf with an effective temperature cooler than $\sim$ 2500K (Sp. type later than M7) and lithium absorption is predicted to have a mass below $0.06M_\odot$: fulfilling the lithium test is a sufficient,but not necessary, condition for substellar mass.

GD 165B: predating the identification of M-type Pleiades brown dwarfs, Zuckerman & Becklin (1989) discovered a companion to the ZZ Ceti white dwarf, GD 165. GD 165B is of indeterminate age (although at least 1 Gyr old), but with known distance and therefore known luminosity: M_K=11.5, M_{bol} = 13.4. The near-infrared colours are extremely red, (J-K)$\sim$ 1.6, and the first spectrographic observations (Kirkpatrick et al, 1993) revealed a spectrum unlike any known late-type M dwarf, with minimal TiO and VO absorption. Treated initially by many as an enigmatic anomaly, GD 165B proves to be the prototype L dwarf. The most recent study (Kirkpatrick et al, 1999a) indicates that the effective temperature is 1900±100K, placing the object in the vicinity of the hydrogen-burning limit.

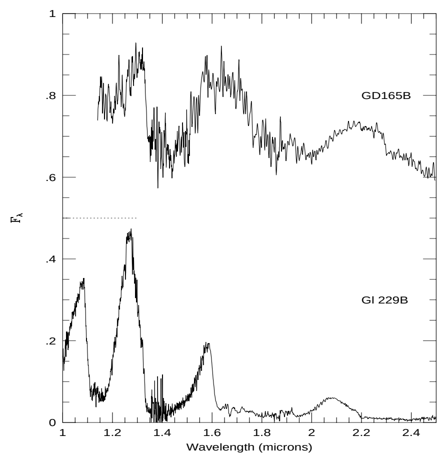

Figure 1: Near-infrared spectra of GD 165B (from Kirkpatrick et al, 1999) and Gl 229B (from Geballe et al, 1996). Note the strong CH_4 absorption at 1.6 and 2.2 μm in the latter object.

Gl 229B: the third harbinger is an object whose distinctive spectrum ensured its immediate acceptance as a substellar-mass brown dwarf. Gl 229B was identified as a common proper motion companion of an M3 dwarf, only $\sim$ 5.5 parsecs distant, through I-band coronagraphic imaging (Nakajima et al,

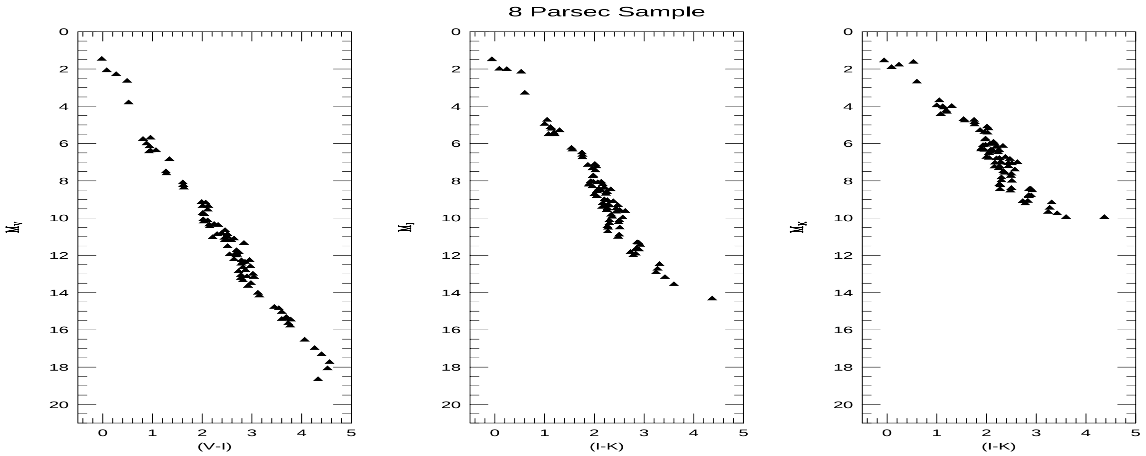

Figure 2: Colour-magnitude relations defined by nearby stars with accurate parallax data - the justification for near-IR surveys.

1995). Although extremely faint, $M_I \sim 21$, infrared photometry showed the companion to have blue JHK colours, with (J-K)$\sim$ 0, comparable to A/F stars. Infrared spectroscopy clarified this conundrum, revealing strong methane absorption in the H and K windows (Oppenheimer et al, 1995; figure 1), a phenomenon predicted 30 years previously by Tsuji (1964) as characteristics of atmospheres cooler than 1200K. At that temperature, Gl 229B in unequivocally not a star, but the first representative of spectral class T. The system is likely to be have an age of at least 1 Gyr, implying a mass of 30 to 60 M_J for Gl 229B. Direct modelling indicates a temperature of $\sim 960 \pm 50$K.

2.2 Results from large-scale surveys

PPl 15 (and other VLM Pleiads), GD 165B and Gl 229B serve as prototypes for brown dwarfs in spectral classes M, L and T, and as a reminder that these objects evolve relatively rapidly for astronomical sources. However, until recently, these were the only such objects known. The crucial breakthrough came, as is the case with many observational projects, with the development and application of new technology, in this case large-scale, high-sensitivity, near-infrared sky surveys.

The justification for searching for VLM dwarfs at near-infrared wavelengths becomes obvious from a cursory consideration of the colour-magnitude diagram described by nearby stars: an M8 dwarf like VB10 is $\sim$ 9 magnitude brighter at K than at visual wavelengths. Infrared surveys had to await the development of array detectors, and even with such detectors, a survey covering 4π steradians requires $\approx 2.1 \times 10^6$ images. Fortunately, infrared detectors have higher DQE than photographic plates, so all-sky surveys to moderate depth are feasible.

Two near-infrared surveys are currently underway: DENIS will cover most of the southern hemisphere, and a small section of the northern equatorial region, to a limiting magnitude (10σ) of I$\sim$ 17, J$\sim$ 15.5 and $K_S \sim 13$ (Epchstein et al, 1994); 2MASS is an all-sky survey, with limiting magnitudes of J$\sim$ 16.5, H$\sim$ 15.8 and $K_S \sim 14.5$. DENIS has the advantage of providing simultaneous optical/IR colours (I-K_S), but has relatively bright limiting magnitudes; 2MASS is more sensitive, but must determine optical-to-IR colours by matching against (non-contemporaneous) IIIaF ($R_{lim} \sim 21$) and IVN($I_{lim} \sim 18.5/19$) data from the POSS II and AAO Schmidt surveys. Putting those new surveys in context, the only previous large-scale near-IR survey, Neugebauer & Leighton's (1969) TMSS, has a limiting magnitude of K$\sim$ 3.

At optical wavelengths, the Sloan Digital Sky Survey represents an order of magnitude improvement in sensitivity over Schmidt photographic surveys. Covering π steradians, SDSS will achieve limiting magnitudes of r'$\sim$ 23.5, i'$\sim$ 22.5 and z'$\sim$ 20.5, with the last dataset for the first time bridging the gap between the optical and near-infrared at $1\mu m$.

The first L dwarfs in the field, three objects spectroscopically similar to GD165B, were detected by the DENIS brown dwarf mini-survey (Delfosse et al, 1997) shortly after that survey commenced in 1996. 2MASS followed with the identification of 20 field L dwarfs (Kirkpatrick et al, 1999b), selected on the basis of their having red near-IR colours ((J-K_S) > 1.3) and no POSS I counterpart (m_r > 20.5, ($m_r - K_S$) > 6). Those objects form the basis of the definition of spectral class L, and a further 65 dwarfs have since been identified from 2MASS data alone.

The early scans made by the Sloan survey also led to the identification of a number of field L dwarfs. More significantly, SDSS follow-up observations of objects with extreme (i'-z') colours produced the first field counterparts to Gl 229B (Strauss et al, 1999). Those two sources were discovered in April and earl-May, 1999; shortly thereafter, Burgasser et al (1999) succeeded in identifying a further 4 examples amongst 2MASS candidates.

3 The new spectral types

Spectral classification provides a shorthand technique for describing the observational characteristics of starlike objects. The main justification for invoking an addition to the standard nomenclature is that the objects identified by DENIS, 2MASS and SDSS fall outwith the descriptive vocabulary of the old system: M dwarfs are defined by the presence of TiO, a species which becomes undetectable in mid- and late L dwarfs. In defining the new class, it is important to use strictly empirical criteria: the assumption is that ordering spectra by their changing appearance provides physical insight, but one should resist the temptation to incorporate preconceptions based on current physical models in setting identification criteria. Similarly, it is a good idea to adopt physically-neutral terminology: Gl 229B-like objects have been called 'methane dwarfs', but methane is expected to be present at detectable levels in the latest L dwarfs. One should draw a clear line between what an object *looks like*, and what an object *is*. The following sections summarise our current understanding of the properties of these objects.

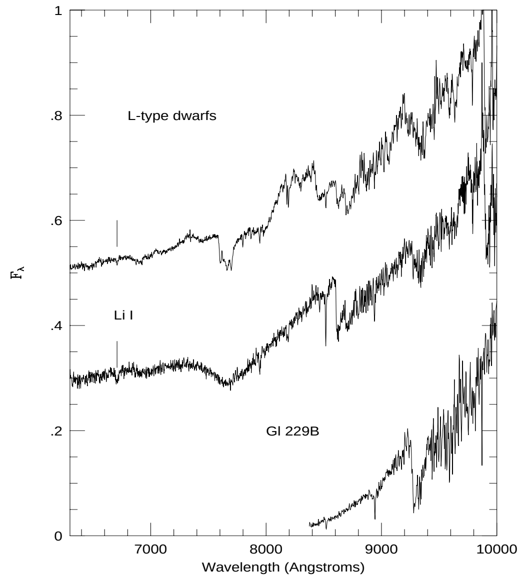

Figure 3: Keck LRIS far-red optical spectra of early-type and late-type L dwarfs. Both have Li 6708Å absorption, implying masses below $0.06M_\odot$. The general characteristics are discussed in the text.

3.1 L dwarfs

Figure 3 plots representative spectra for an early (L1) and late (L7) L dwarf. As noted above, the most obvious change relative to M dwarfs is the reduction in TiO and VO bandstrength. TiO weakens and disappears, save for the λ8432Å band, at ~L2; VO at ~L5. The most prominent molecular bands are metal hydrides, CaH, FeH, CrH and (at shorter wavelengths) MgH, while strong atomic lines due to Cs, Rb, Na, K and, sometimes, Li are also present. The latter lines grow in strength at later spectral types (i.e. lower temperatures), with the K I doublet at 7665/7699Å showing a dramatic increase in equivalent width beyond ~L6. The sodium D lines exhibit similar behaviour between L3 and L5, with the wings spanning over 1000Å in the latter dwarfs (Reid et al, 2000). The spectra become increasingly smooth, and by spectral class T, the only features evident are the 8521, 8943Å Cs I lines and strong H_2O absorption at $\sim$ 9250Å.

Our spectral classification system is based solely on the changing morphology of the spectra. However, increasing spectral type L0 to L8 also corresponds to redder optical/IR and near-IR colours (figures 4 and 5), indicating that increasing spectral type corresponds to decreasing effective temperature. The accepted physical interpretation of the spectral changes evident in figure 3 is that we are seeing the effects of dust formation within the atmospheres of these cool dwarfs. This process was originally identified as important by Tsuji et al (1996), who showed that the long-standing discrepancy between the predicted and observed strengths of the near-IR H_2O bands could be resolved if dust heats the upper atmosphere in late M dwarfs, weakening the bandstrength. The

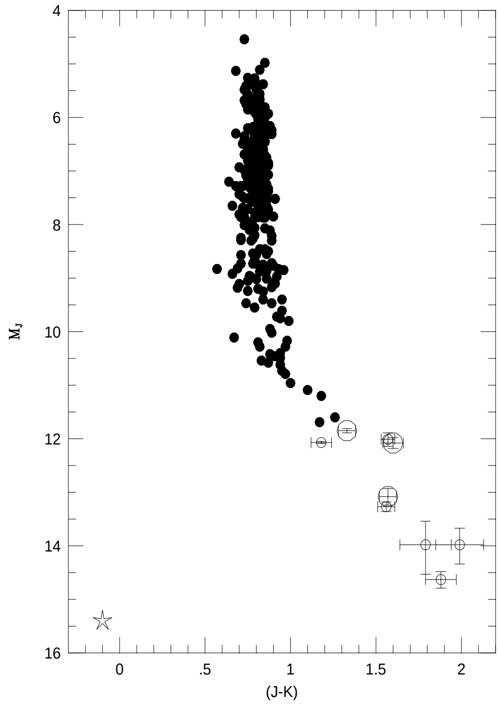

Figure 4: The (M_J, (J-K_S)) colour-magnitude diagram for M, L and T dwarfs. Trigonometric parallaxes for the L dwarfs plotted here were determined by the US Naval Observatory (Dahn et al, in prep.).

complex process of dust formation has been considered by a number of groups (Fegley & Lodders, 1996; Burrows & Sharp, 1999; Allard, Chabrier, Baraffe et al, in prep.). While details remain to be determined, the concensus is that TiO first stars to condense as calcium titanate at $T_{eff} \sim$ 2500K (spectral type M6/M7), VO solidifies at close to 1900K, and other species condense at still lower temperatures (Table 1). Comparing theoretical predictions against observations allows one to infer an approximate temperature scale for L dwarfs, with upper and lower limits of $\sim$ 2000K for L0 and $\sim$ 1300K (1200K?) for the as-yet unobserved type, L9.

Molecule	dust constituent	depletion temperature
TiO	$CaTiO_3$	≈1900/2000K, L2
VO	solid VO	1700 to 1900K, L4
Na	high albite	1200-1300K, L9?
	NaCl	≈ 1150K, T?
CrH	metallic CrH	~ 1400K, L8
Li	LiCl	<1400K, >L8
Rb, Cs, K	RbCl, CsCl, KCl	<1200K, >L8
CO	CH_4	~1250K?, L/T transition

Table 1: Dust formation in M, L, T dwarfs

As dust formation removes molecular TiO and VO from the atmosphere, the opacity is reduced. This leads to the increased strength in the alkali lines, due both to the substantial column densities to $\tau = 1$ and to the high gas pressures at the formation level. The latter effects are particularly evident in the high abundance species, Na and K, and account for the dramatic broadening of the D lines, a resonance doublet, at spectral type L5. The resultant white dwarf-like absorption lines absorb a substantial fraction of the V-band flux, leading to jump of $\sim$ 1 magnitude in the (V-I) colour between spectral types L4 and L5. Similar effects are evident in the (I-J) colour over the L/T transition due to broadening of the KI 7665/7699Å resonance doublet (Kirkpatrick et al, 1999b; figure 5).

3.2 T dwarfs

All brown dwarfs eventually cool to the point where the spectral energy distribution matches that of Gl 229B: a near-infrared spectrum characterised by strong CH_4 overtone absorption in the H and K windows. Identifying these low-luminosity dwarfs (Gl 229B has $M_K \sim 15.5$ and $M_I \sim 22.5$) in infrared surveys is complicated by the blue JHK colours, comparable with A/F stars. In contrast, the optical/IR colours are unique to this type of object (figure 5), although one should note that both of the SDSS T dwarfs have i'$\sim$ 23.5, below the survey limit. In both cases, however, the z' magnitude is comfortably within the nominal survey parameters. Thus, deep optical surveys, such as SDSS, have the advantage of searching for objects with extreme colours, but at very faint apparent magnitudes; near-infrared surveys, such as 2MASS, target brighter apparent magnitudes, but must sift through a much larger number of contaminants. The latter process is undertaken by matching 2MASS sources against POSS II/UKST plate material and identifying 'blue' JHK sources with no optical counterpart. Unfortunately, since the optical and infrared data are not contemporaneous, that still leaves a large population of uncatalogued moving objects (mainly asteroids) and early/mid-type M dwarfs, just below the photographic plate limit. Those sources must be eliminated through repeat JHK imaging (see Burgasser et al, 1999 for full details). Clearly, the optimum search method will be combining the SDSS and 2MSS datasets and using the (z-J) colour as the prime T dwarf identifier.

Two key questions in interpreting the available observations to estimate $\Psi(M)$ are: what is the temperature of the L/T transition? and how rapidly does CH_4 absorption increase in strength. With only six field T dwarfs known, plus Gl 229B, our answers are at best sketchy at present, but low-resolution near-IR spectra suggest that the field T dwarfs are somewhat hotter than Gl229B. One expects a magnitude-limited areal survey to preferentially select higher luminosity sources, and since there is little dispersion in radius amongst brown dwarfs, the most luminous sources should also have the higher temperatures.

There are also indications that the L/T transition is relatively rapid. First, extensive follow-up observations of neutral-coloured (JHK) 2MASS sources have failed to identify any transition sources; second, SDSS, which has the advantage of a monotonically-varying colour, has identified L dwarfs, T dwarfs, but no transition sources; theoretical predictions (Allard et al, in prep.) predict a rapid transition; and, finally, and most convincingly, the latest L dwarfs (L8+) are only 0.5 to 0.8 magnitudes brighter in M_J than Gl 229B. While one must allow for the fact that these atmospheres are extremely non-grey, this small offset suggests a comparably small offset in M_{bol} and effective temperature. In Table 1, I suggest that the L/T transition may lie in the 1200-1300K temperature range.

4 $\Psi(M)$ at substellar masses

Constraining the form of the mass function below the hydrogen burning limit is not a straightforward process, even given the plentiful new observations of ultracool dwarfs in the field. Brown dwarfs evolve along similar (L, T_{eff}) evolutionary tracks, but at mass-dependent rates. As a result, there is no mass-luminosity relation, as with stable, fusion-powered stars. Our only recourse is to model the observed (apparent magnitude, spectral type) distribution by folding (L, T_{eff}) predictions from theoretical models with estimates of $\Psi(M)$ and the stellar birthrate, B(t), and transforming the results to the observational plane. Given the mass dependence of the evolutionary rates, decoupling $\Psi(M)$ and B(t) is extremely difficult. Nonetheless, the first attempt at this type of analysis has been undertaken by Reid et al (1999). Before discussing

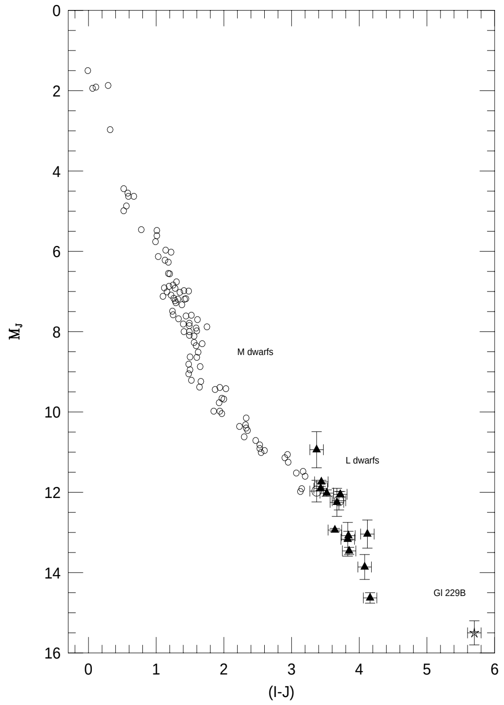

Figure 5: The (M_J, (I-J)) colour-magnitude diagram for M, L and T dwarfs, illustrating the greater effectiveness of optical-IR colours in identifying T dwarfs. Note the $\sim$ 1.5 magnitude offset in (I-J) between Gl 229B and the latest L dwarf (sp type L8).

those results, two related considerations require consideration.

4.1 The stellar mass function

The zeropoint for the substellar simulations rests on the inferred density of stars above the hydrogen-burning limit, since we assume that the star formation process is not cognisant of astrophysical requirements for fusion. The most reliable method of determining that parameter is through a census of the nearest stars: we favour using stars within 8 parsecs, north of -30o: a total of 103 systems, 100 of which have accurate trigonometric parallaxes and almost all of which have been surveys for multiple companions. The mass function derived from those data is consistent with a power-law, $\Psi(M) \propto M^{-1.13\pm0.15}$ for stars; $\Psi(M) \propto M^{-0.9\pm0.15}$ for systems.

4.2 Binarity

Photometric surveys are biased in several ways by the presence of binaries: equal-mass systems are over-represented, but low luminosity companions at small separations are difficult to detect. The binary fraction amongst disk dwarfs is traditionally quoted as $\sim$ 50%, but that value is based on observations of G dwarfs. The binary fraction amongst M dwarfs is closer to $\sim$ 35% (Fischer & Marcy, 1992; Reid & Gizis, 1997). As yet, no good statistics are available for low-luminosity L dwarfs, although several are known to be in binary systems. Four L dwarfs are wide companions of nearby bright stars: G196-3 (Rebolo et al, 1998); GL 1001B (or LHS 102B, Goldman et al, 1999); and two 2MASS sources (Kirkpatrick et al, in prep.). In addition, four L dwarfs are known to be binaries with nearly equal-mass components: DENIS1228 (Martín et al, 1999) and 2M1146 (Koerner et al, in prep.) are both resolved systems, separation $\sim$ 0"3; PPl15 and 2M0345 (Reid et al, 1999) are both double-lined spectroscopic system. If the binary fraction, and mass ratio distribution, is comparable to that amongst L dwarfs, the effects on the inferred $\Psi(M)$ are relatively minor.

4.3 $\Psi(M)$ below the hydrogen-burning limit

The initial analysis outlined by Reid et al (1999) considered a K-band magnitude-limited sample, which is reasonable for M and L dwarfs. The 1.25μm methane-free J band, however, is clearly the optimum choice for calculations incorporating T dwarfs, since the available data suggest that the bolometric correction, BC_J, varies by only 0.1 to 0.2 magnitudes from $T_{eff} \sim 2800$K (M6: Gl 406) to ~ 1000K (Gl 229B). The observational constraints are set by the observed surface density of L dwarfs, ≈ 1 per 20 square degrees, or 2000 all-sky, to J=16; and the T dwarf surface density of ≈ 1 per 400 square degrees, or ≈ 100 all-sky, to the same magnitude limit. The model assumes a constant birthrate over the history of the Galactic disk (age 10 Gyrs) and a power-law mass function, $\Psi(M) \propto M^{-\alpha}$, where $\alpha = 2.35$ is the Salpeter function.

There are two critical temperatures for the simulations: the transition between type M and L, T_{ML}; and between types L and T, T_{LT}. Theoretical models suggest that the former transition lies close to 2000K. Given T_{ML}, we can predict the total number of L and T dwarfs with apparent J magnitudes brighter than 16 for a given value of α, while the relative number of L and T dwarfs, $\frac{N_T}{N_L}$, depends on T_{LT}. The former predictions are ~ 200 L+T dwarfs for $\alpha = 0$; ~ 900 L+T dwarfs for $\alpha = 1$; and ~ 5500 for $\alpha = 2$. The observations favour $1 < \alpha < 2$. Figure 6 plots $\frac{N_T}{N_L}$ as a function of T_{LT} for $\alpha = 1, 2$. With an observed value of $\frac{N_T}{N_L} \sim 5\%$, this comparison suggests a transition temperature below 1200K.

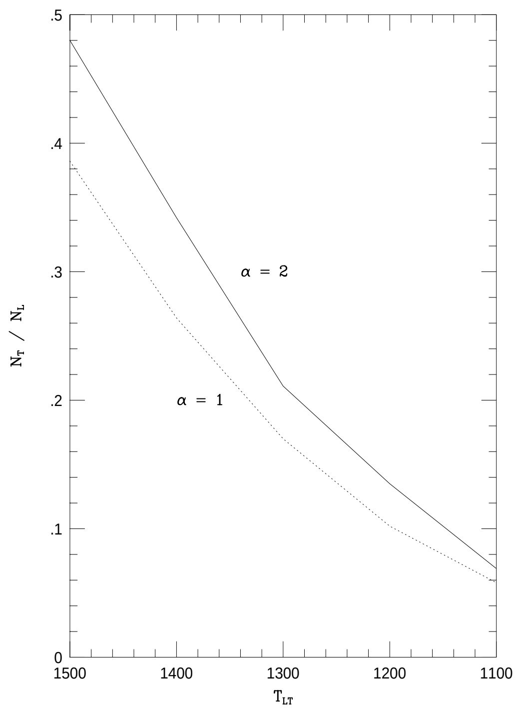

Figure 6: The relative number of L and T dwarfs as a function of the L/T transition temperature for power-law mass functions with $\alpha = 1$ and $\alpha = 2$.

The lithium test provides a further probe of $\Psi(M)$. Since the observed L dwarf (and T dwarf) sample should span the full range of masses below $\sim 0.09 M_\odot$, the relative number of dwarfs with and without lithium absorption provides a measure of the relative numbers above and below $0.06 M_\odot$. If $\alpha = 2$, two-thirds of the sample are expected to have detectable Li 6708Å; if $\alpha = 1$, the fraction is $\sim \frac{1}{3}$ Current observations place the relative numbers as closer to the latter fraction, suggesting $\alpha \sim 1$. This is also broadly consistent with the latest surveys of the brown dwarfs in the Pleiades cluster (Bouvier et al, 1998), although mass segregation and subsequent evaporation of low-mass stars is a concern in open cluster analyses, even for an intermediate-aged cluster like the Pleiades. J. Adams and collaborators are currently analysing 2MASS scans of this cluster, and, combined with POSS II material, those data will provide a thorough determination of mass segregation effects.

Clearly, the present results are very preliminary. In general, however, the results are not inconsistent with a smooth extrapolation of the stellar mass function into the brown dwarf régime. Under those circumstances, brown dwarfs outnumber stars by almost a factor of 2 to 1, nut contribute less than 10% of the stellar mass density. The median temperature of the local brown dwarf population is ~ 400K, and the few L and T dwarfs discovered to date represent the tip of a very large iceberg.

5 Subdwarf and the halo mass function

With an age of 10-14 Gyrs, there is little possibility of detecting significant numbers of brown dwarfs in the metal-poor Galactic halo,. However, recent observations of low-mass subdwarfs in both globular clusters and the general field have led to improved estimates of the form of the mass function close to the hydrogen-burning limit. Since this population has a metal abundance substantially below that of the typical star in the Galactic disk, these new observations provide a test of the hypothesis that the stellar mass function is universal.

HST observations have proven crucial in extending the range and accuracy of luminosity function determinations in Galactic globular clusters. NGC 6397 provides the poster-child of cluster colour-magnitude diagram studies, with proper motions derived over a baseline of only two years leading to clean discrimination between members and background/foreground contamination (King et al, 1997). Unfortunately, that cluster represents a poor choice for measuring $\Psi(M)$ since there is strong evidence for substantial dynamical evolution and evaporation of low-mass stars. More distant, but less perturbed, outer halo clusters, such as M15, M55 and M30, are better suited to this type of analysis, although modest corrections to $\Psi_{obs}(M)$ are require in even those clusters (Piotto & Zoccali, 1999). Analyses generally derived mass functions which are somewhat steeper than the disk mass function: matched against a power-law, the indices lies in the range $-1.2 < \alpha < -1.5$.

Analysis of field subdwarfs leads to similar conclusions. The identification of these stars still rests on the time-honoured technique of proper motion surveys: since halo stars have, on average, higher tangential velocities (relative to the Sun) than disk dwarfs, they are over-represented (relative to their volume density) in proper motion surveys. Low luminosity subdwarfs can be distinguished from their solar-abundance counterparts based on the relative strengths of TiO and metal hydride bands (mainly MgH and CaH), and Gizis (1997) has established a spectral sequence which permits a crude abundance estimate. The observed numbers of proper motion stars depends on the assumed halo kinematics, but there are well established techniques for allowing for the associated kinematic bias (Bahcall & Casertano, 1986). Thus, the halo luminosity function can be derived in a relatively straightforward manner (Dahn et al, 1994; Gizis & Reid, 1999).

The transformation from $\Phi(M_V)$ to $\Psi(M)$ is complicated by the fact that the mass-luminosity relation is a function of abundance and lacks direct empirical calibration. Figure 7 shows preliminary results from analysis of the available proper-motion data (Reid & Gizis, in prep.). The data suggest a mass function with $\alpha \sim 1.5$, steeper than the disk function, but not inconsistent with globular cluster data. This suggests a possible correlation between $\Psi(M)$ and [m/H], a matter of importance for both star formation theory and cosmology.

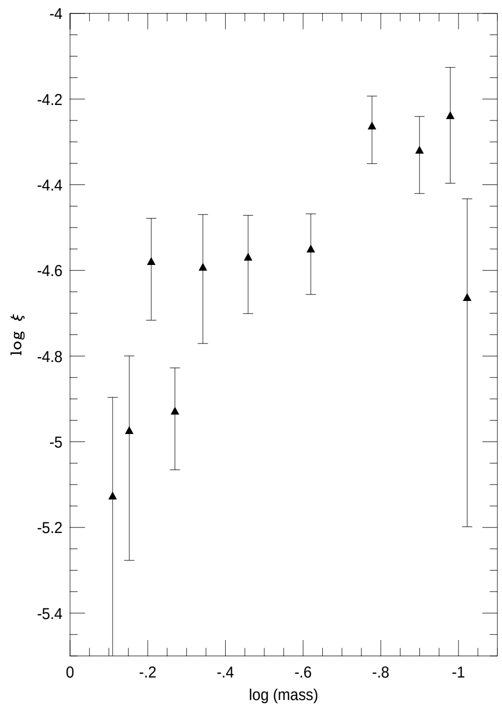

Figure 7: $\Psi(M)$ for the Galactic halo, derived from analysis of proper motion stars. A Salpeter function has slope 1.35 in this diagram; $\alpha = 1$, the disk function, has slope zero.

6 Conclusions

Initial results from the new generation of near-infrared (DENIS, 2MASS) and optical (SDSS) surveys have revolutionised studies of substellar-mass objects. Five years ago there were no universally-accepted brown dwarfs; now we have almost 100 examples, two new spectral classes and a moderately-understood evolutionary sequence. Deconvolving the underlying mass function is a process not without pitfalls, but preliminary analysis suggests that the available observations are not inconsistent with a simple extension of the stellar mass function, $\Psi(M) \propto M^{-1.1}$, to substellar masses. In contrast, the current best estimates of $\psi(M)$ for the Galactic halo suggest that those metal-poor stars follow a somewhat steeper function, with $\alpha \approx 1.5$. Further observational and theoretical work as we enter the final year of the twentieth century (2000) should shed new light on these important questions.

Acknowledgements

I would like to congratulate the LOC/SOC of Star Formation 99 for organising an extremely successful meeting. Many of the results discussed in this review were made in collaboration with members of the 2MASS Rare Objects Team Key Project: Davy Kirkpatrick (IPAC), John Gizis (UMASS), Jim Liebert (UA), Adam Burgasser (Caltech), Conard Dahn and Dave Monet (USNO), and Chas Beichman (JPL). This work is funded partially by a NASA/JPL grant to 2MASS Core Project science.

References

Bahcall, J.N., Casertano, S. 1986, ApJ, 308, 347
Basri, G., Marcy, G.W., Graham, J.R. 1996, ApJ, 458, 600
Basri, G., Martín, E.L. 1998, Brown dwarfs and extrasolar planets, ASP Conf. Ser. 134, ed. R. Rebolo, E.L. Martín, M.R. Zapatero-Osorio, p. 284
Bouvier, J., Stauffer, J.R., Martín, E.L., Navascues, D.B.Y., Wallace, B., Bejar, V.J.S., 1998, A&A, 336, 490
Burgasser, A.J., Kirkpatrick, J.D., Brown, M.E., Reid, I.N et al, 1999, ApJL, 522, L
Burrows, A., Sharp, C.M. 1998, ApJ, 512, 843
Dahn, C.C., Liebert, J.W., Harris, H., Guetter, H.C. 1995, in The Bottom of the Main Sequence and Beyond, ed. C.G. Tinney, (Heidelberg: Springer), p. 239
Delfosse, X. et al 1997, A&A, 327, L25
Epchtein, N. et al, 1994 in Science with Astronomical Near-Infrared Surveys, Ap. Sp. Sci, 217, 3
Fegley, B., Lodders, K. 1996, ApJ, 472, L37
Fischer, D.A, Marcy, G.W. 1992, ApJ, 396, 178
Geballe, T. et al 1996, ApJ, 467, L101
Gizis, J.E. 1997, AJ, 113, 806
Gizis, J.E., Reid, I.N. 1999, AJ, 117, 508
Goldman, B., Delfosse, X., Forveille, T., the EROS collaboration 1999, A & A, in press
King, I.R., Anderson, J., Cool, A.M., Piotto, G. 1998, ApJ, 492, L37
Kirkpatrick, J.D., Henry, T.J., Liebert, J. 1993, ApJ, 406, 701
Kirkpatrick, J.D., Allard, F., Bida, T., Zuckerman, B., Becklin, E.E., Chabrier, G., Baraffe, I. 1999a, ApJ, 519, 834
Kirkpatrick, J.D., Reid, I.N., Liebert, J., Cutri, R., Nelson, B., Beichman, C.A., Dahn, C.C., Monet, D.G., Skrutskie, M.F., Gizis, J.E. 1999b, ApJ, 519, 802
Martín, E.L., Brander, W., Basri, G. 1999, Science, 283, 1718
Nakajima, T., Oppenheimer, B.R., Kulkarni, S.R., Golimowski, D.A., Matthews, K., Durrance, S.T. 1995, Nature, 378, 463
Oppenheimer, B.R., Kulkarni, S.R., Matthews, K., Nakajima, T. 1995, Science, 270, 1478
Piotto, G., Zoccali, M. 1999, A&A, 345, 485
Rebolo, R., Martín, E.L., Maguzzu, A. 1992, ApJ, 389, L83
Rebolo, R., Zapatero Osorio, M.R., Madruga, S., Bejar, V.J.S., Arribas, S., Licandro, J. 1998, Science, 282, 1309
Reid, I.N., Gizis, J.E. 1997, AJ, 113, 2286
Reid, I.N., Kirkpatrick, J.D., Liebert, J., Burrows, A., Gizis, J.E., Burgasser, A., Dahn, C.C., Monet, D., Cutri, R., Beichman, C.A., Skrutskie, M. 1999, ApJ, 521,
Stauffer, J., Hamilton, D., Probst, R., Rieke, G., Mateo, M., 1989, Apj, 344, L21
Stauffer, J., Hamilton, D., Probst, R.G. 1994, AJ, 108, 155
Tsuji, T. 1964, Ann. Tokyo Obs. ser. II, 9, 1
Tsuji, T., Ohnaka, K., Aoki, W. 1996, A&A, 305, L1
Zapatero-Osorio, M.R., Rebolo, R., Martín, E.L., Basri, G., Magazzu, A., Hodgkin, S.T., Jameson, R.F., Cossburn, M.R. 1997, ApJ, 491, L81
Zuckerman, B,. Becklin, E.E. 1988, Nature, 336, 656

Star Formation 1999, June 21–25, 1999, Nagoya, Japan